Available online at www.sciencedirect.com
ScienceDirect
Journal of Power Sources 179 (2008) 592–602
JOURNAL OF POWER SOURCES
www.elsevier.com/locate/jpowsour

Investigations on thermo-mechanical fabrication of micro-scale porous surface features

Muammer Koç *, Yusuf Usta, Alp Karakoç

NSF I/UCR Center for Precision Forming (CPF) & Department of Mechanical Engineering, Virginia Commonwealth University (VCU), Richmond, VA, USA

Received 26 November 2007; received in revised form 22 January 2008; accepted 23 January 2008
Available online 7 February 2008

Abstract

In this paper, we present the preliminary results of our investigations to fabricate porous micro-feature surface structure arrays on large surface areas for fuel cell and other heat/mass transfer applications. We hypothesized that micro-channels of around 200–400 μm height and width with porosity levels of 30–50% and with strong bonding to a thin substrate could be fabricated using hot powder compaction and/or hot roll powder compaction. We investigated the effects of compaction pressure, temperature, holding time, powder size and substrate conditions on the attainable porosity and channel size. Our feasibility study findings indicate that both pressure and temperature have significant effect on the porosity level. Suggested temperature levels are around 450 °C to ensure strong bonding among powders and between powders and the thin substrate. Minimum pressure level can be around 50 MPa, but it depends on the temperature levels. Roughened substrate surface condition is found to slightly assist in achieving strong bonds and high porosity. In order to have high porosity levels, uniform powder size is preferred. Although not tested extensively, hot compacted specimens up to 450 °C temperature levels are found to be not very strong. Hence, subsequent sintering is necessary.

Keywords: Fuel cell; Bipolar plate; Interconnect plate; Porous surfaces; Powder forming; Micro-manufacturing

1. Introduction

One of the basic elements of fuel cell stacks is the heat and mass transfer plates known as either bipolar plates in PEMFCs or interconnect plates in SOFCs. Their main functions are to (1) equally distribute the gases (hydrogen and oxygen) to anode and cathode surfaces for electrochemical reactions, (2) structurally support the MEA and (3) transmit the electrons [1–5]. Thus far, various methods are developed to fabricate such plates addressing their needs for efficient flow field designs, weight and volume, contact resistance and cost. For the bipolar plates, currently, three methods or types are commonly used, tested and promoted: (1) metallic bipolar plates mostly made of stainless steel alloys [6], (2) composite bipolar plates [3,7–9] and (3) graphite bipolar plates [10]. For the interconnect plates, based on the type of SOFC whether it is an anode supported, electrolyte supported or interconnect-supported, there are various ways of fabrication and materials. For the interconnect-supported type, micro-channeled stainless steel alloys are being developed as they promise a remarkable cost reduction [4,5]. Regardless of whether it is a PEMFC or SOFC, in order to increase the efficiency of fuel cells, reduce weight and cost, alternative surface structures on these plates have been developed. Micro-scale porous surface texture on the metallic bipolar/interconnect plate can enhance the thermal and chemical reaction properties, and hence, increase the efficiency and performance of fuel cell (i.e., kW/weight or kW/volume). The benefit of such innovative plate concept utilizing porous surface structure has been demonstrated previously using metallic foams [11–13]. However, the cost of such thin foams is high, and only passive control of the porosity is possible. Modulated porous surfaces at micro-scales (i.e., micro-channels or micro-bump arrays on a large surface) were found to enhance the heat transfer efficiency up to 300% [14] when compared to plain surfaces as depicted in Fig. 1. It was reported that functionally engineered surfaces with micro-scale features and porosity can enhance the heat/mass transfer mainly by offering (a) increased surface area in a given volume and mass, (b) capillary-assistance to liquid flow effect, (c) increased

* Corresponding author. Tel.: +1 804 827 7029.
E-mail address: mkoc@vcu.edu (M. Koç).

0378-7753/$ – see front matter © 2008 Elsevier B.V. All rights reserved.
doi:10.1016/j.jpowsour.2008.01.056

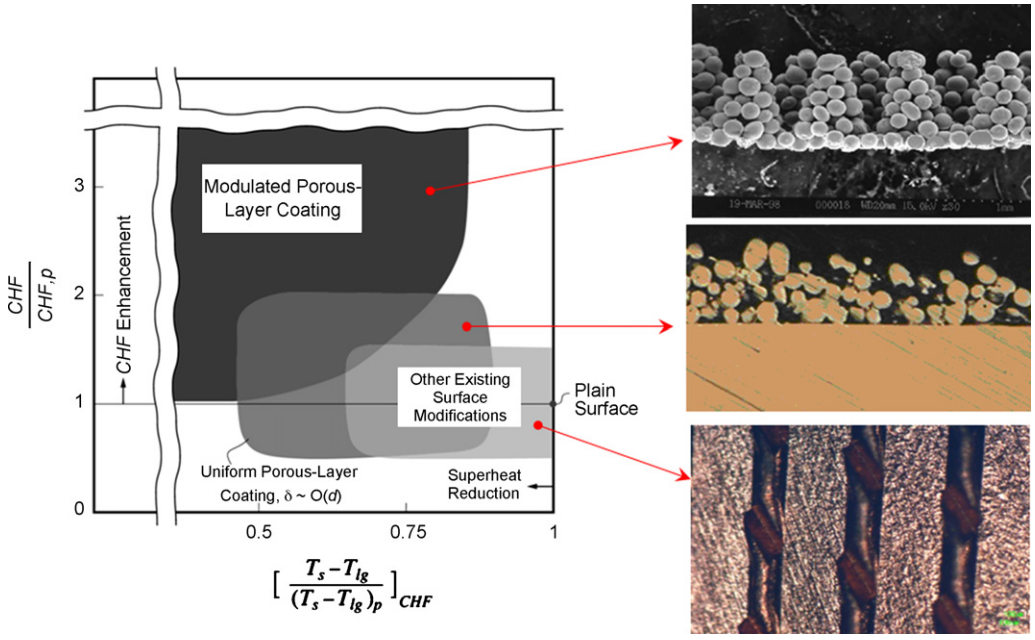

Fig. 1. Enhancement of heat transfer efficiency by using modulated porous surfaces (i.e., micro-features with porosity) [14].

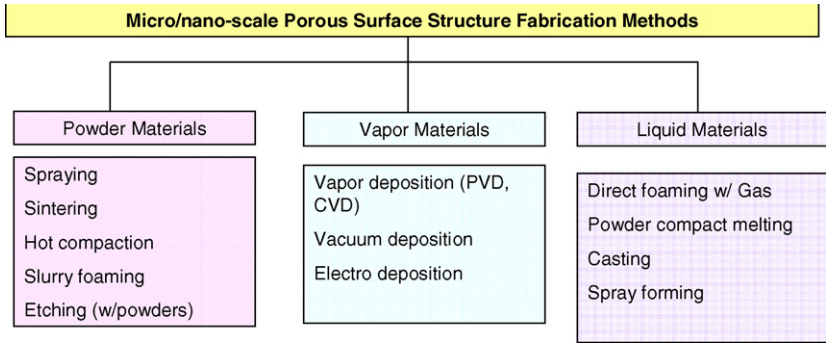

Fig. 2. Classification of porous surface fabrication methods [25–27].

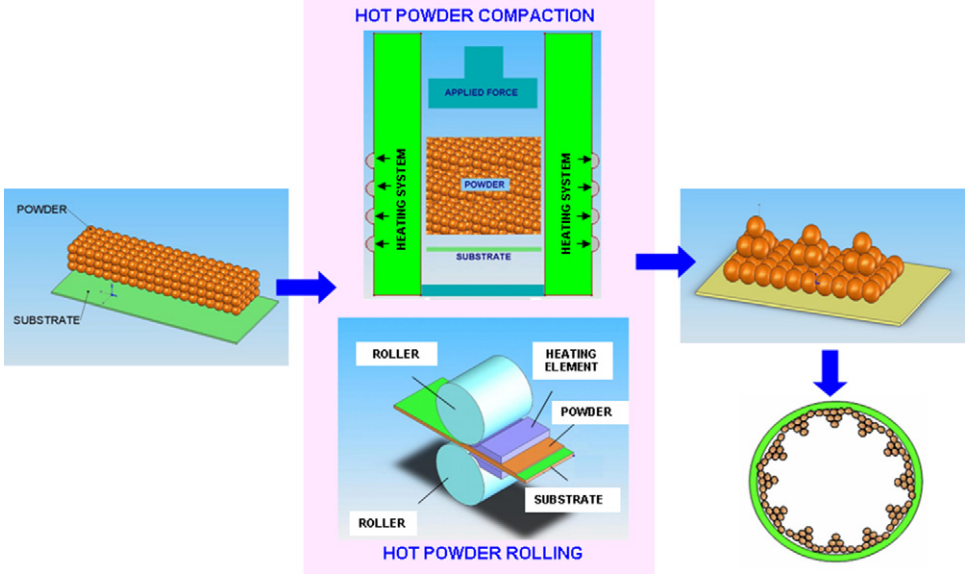

Fig. 3. Fabrication of modulated porous micro-scale surface features.

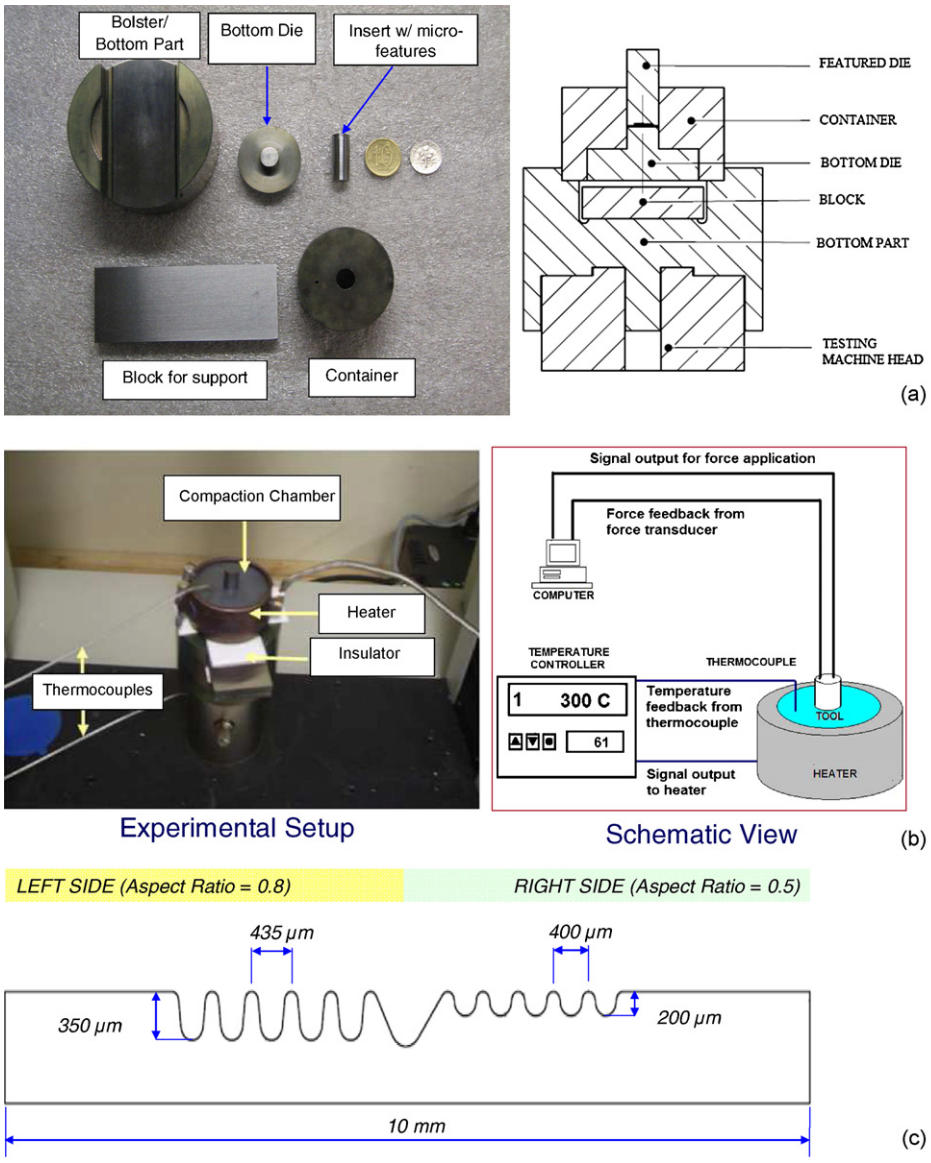

Fig. 4. (a) Experimental tooling, (b) heating and temperature control system and (c) size and geometry of the micro-channels.

Table 1
Experimental conditions for each phase

Experiments	Conditions	Values	Explanation
Phase 1	Temperature	20, 110, 150, 300 and 450 °C	
	Pressure	250 and 320 MPa	
	Holding time	10 s	
	Substrate	Cu 110, t_o = 100 μm smooth and rough	Rough surfaces are obtained by brushing with sand paper
	Powder	Average size: 50 μm,	(10% < 25 μm, 50% < 50 μm and 90% < 100 μm)
Phase 2	Temperature	300 and 450 °C	
	Pressure	50, 70, 100, 150 and 200 MPa	
	Holding time	30, 60 and 120 s	
	Substrate	Cu 110, t_o = 100 μm rough surface	
	Powder	Average size: 50 μm,	(10% < 25 μm, 50% < 50 μm and 90% < 100 μm)
Phase 3	Temperature	450 °C	
	Pressure	50 MPa	
	Holding time	60 s	
	Substrate	Cu 110, t_o = 100 μm rough surface	
	Powder	Average size: 50 μm	More uniform (45–53 μm)

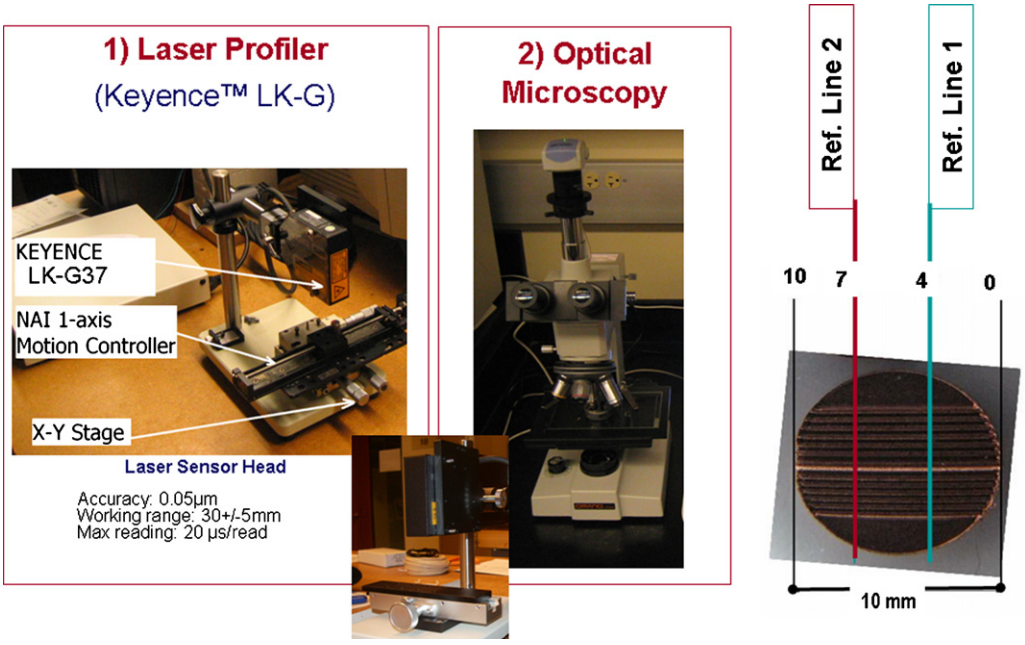

Fig. 5. Methods and procedure used for measurement of channel heights. (1) laser profiling methods and (2) optical microscopy.

nucleation site density, (d) enhance vapor escape paths and (e) increased catalyst loading capacity [14]. This type of surfaces can also find applications in fuel processor or reformers to obtain high purity hydrogen [15] and biomedical devices [16].

Since the cost is a major issue in commercial and affordable realization of fuel cells, any fabrication technique for any of fuel cell component should be economically justified. Thus, only a few of the existing methods are likely candidates to fabricate porous surfaces for fuel cell applications under the mass production and low-cost requirements. Existing methods of fabricating porous structures can be classified according to the state of the material during processing, which defines four "families" of processes as follows: (1) liquid material, (2) powder material, (3) metal vapor or gaseous metallic compounds, (4) metal ion solution, Fig. 2 [17–19]. Among them, powder or fiber sintering is a commonly used method for many other applications such as filtration, lubrication, etc. [20–21]. Kartsounes used copper plasma spray for coating, while Dahl and Erd [22] employed a flame powder spray method. Some researcher employed electroplating (electro-deposition) technique for porous-layer coating. For example, Fuji et al. [18] made a micro-porous surface by fixing copper particles on a smooth flat surface by plating with copper, and Janowski et al. [23] invented a way by attaching a porous reticulated organic foam layer to a tube and then plating

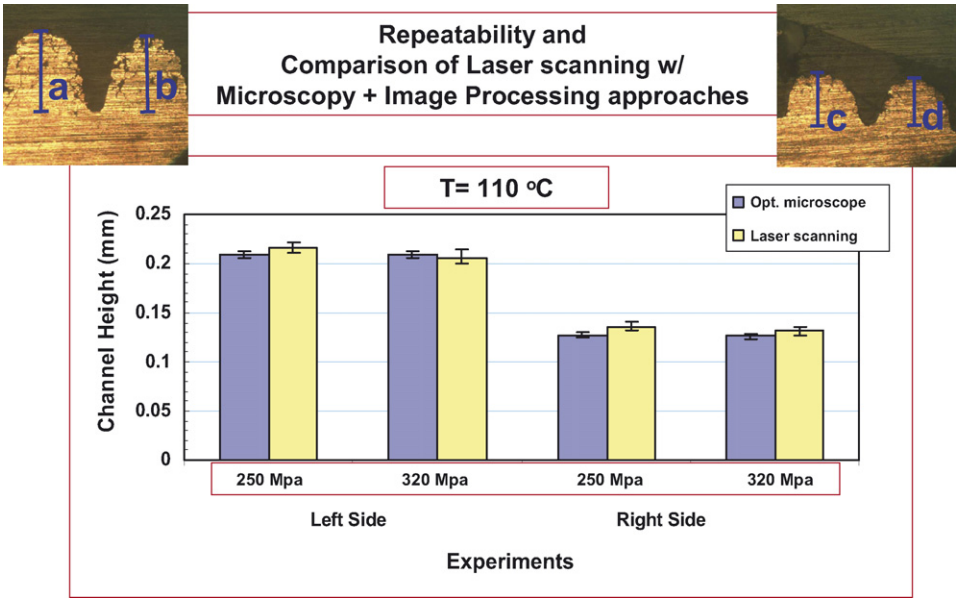

Fig. 6. Comparison of channel height measurements obtained by optical microscopy and laser profiling methods.

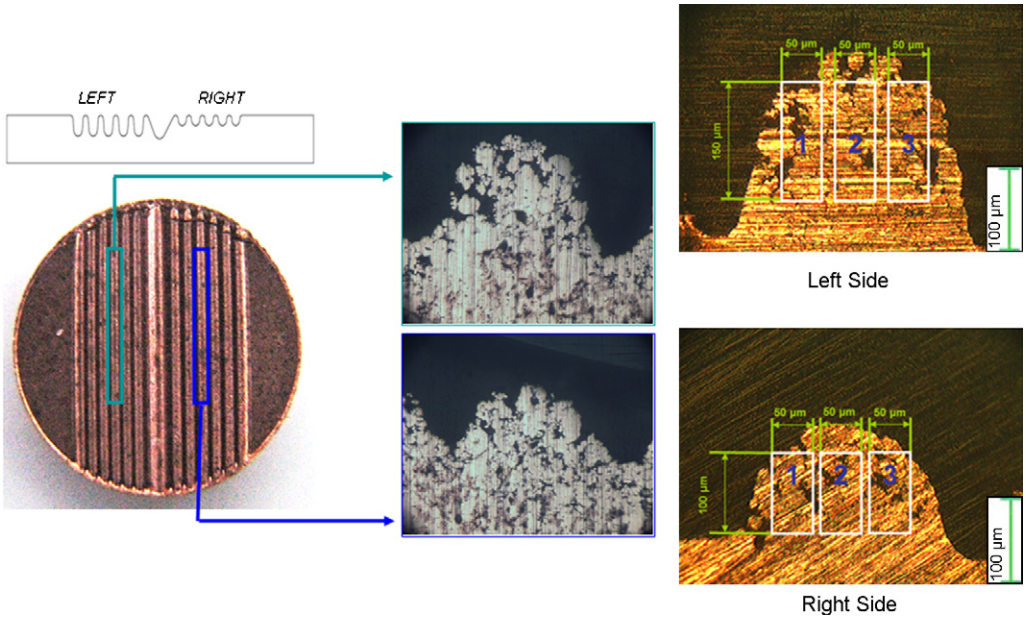

Fig. 7. Porosity measurement procedure and sample results.

a thin metal coating on the foam. Kunugi et al. [24] developed a chemical etching method as discussed in the previous section. As demonstrated in their study, a nanoparticle porous layer can be formed on a substrate surface by etching with some acids or alkalis including around 100 nm size nanoparticles made from copper oxide, carbon nanotube and aluminum oxide. However, in summary, all of the above methods suffer from mass and cost-effective manufacturing difficulties since it is a multi-step procedure and requires longer cycle time. Due to its simplicity and low operating cost, compaction of particulate materials has been used for a large number of applications in mining, mineral, metallurgical, chemical, food and pharmaceutical industries. Typically, fine powders are compacted by mechanical pressure exerted by either flat plates or rolls. Rolling process has also been used to establish the atom-to-atom bond between two pieces to be joined through intimate contact by mechanical pressure, which is called 'roll bonding'. The main advantage of hot compaction and/or rolling is that very high pressure can be exerted in a productive manner as illustrated in Fig. 3.

In this study, we aimed to develop a novel manufacturing process based on hot powder compaction to fabricate porous surfaces with modulated micro-scale features on a thin solid substrate for heat/mass transfer enhancement. The primary goal of this feasibility study was to understand if micro-features with porosity could be fabricated under different temperature and pressure conditions to control the feature size ad porosity. We defined three major important aspects for the desired surfaces: (1) micro-scale features (i.e., modulated channels or bumps), (2) interconnected and controlled porosity, and (3) mechanically strong and minimal thermal-resistant bonding with a solid thin substrate. In order to assess the manufacturability, process control (i.e., pressure versus porosity and temperature versus porosity) and robustness issues, in this preliminary phase of our studies, we used copper powders as they can be formed at lower temperature and pressure levels compared to stainless steel, which is a preferred type of material particularly for electrochemical stability in fuel cell applications. Moreover, copper was chosen to address micro-compaction of porous surfaces for heat exchanger applications. We expected that our findings with copper powder compaction would guide us through the second phase studies where we intend to use stainless steel powders.

In this paper, after presenting the overall motivation, objectives and state-of-the art review of fuel cell component manufacturing in the introduction section, we described the experimental methodology, tooling and measurements in Section 2. In Section 3, we presented the experimental results and discussed their analyses. In Section 4, we summarized our findings and laid out a plan for the future work.

2. Description of experimental tooling, method and measurements

We conducted our feasibility experiments in three phases using the same tooling under different conditions. We investigated the feature size (i.e., channel height and micrometer), porosity (%) and bonding quality with the thin substrate as a function of temperature (room temperature to 450 °C), compaction pressure (25–320 MPa), substrate surface condition (smooth or rough), powder size distribution (average 50 μm with varying minimum values) and compaction time (0–120 s).

2.1. Experimental tooling and system

Compaction experiments were conducted on a 30 kN MTS machine. We were able to apply and control the pressure with this MTS Insight 30 machine. A compaction tooling (Fig. 4a) consisting of a bolster, bottom die, insert with channel geometry and container was manufactured using H13 tool steel material to enable hot compaction experimentation. During the hot com-

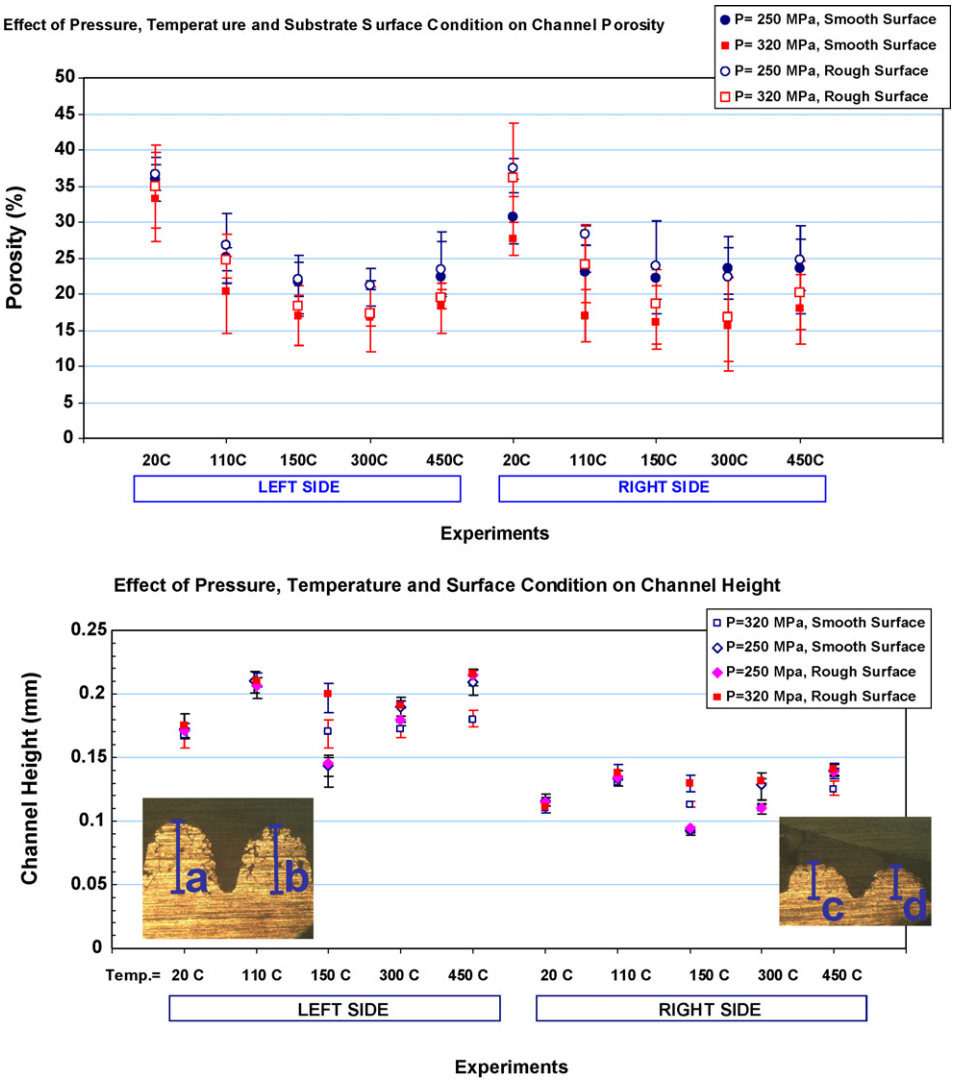

Fig. 8. Variation of porosity (a) and channel height (b) at different temperature levels (20, 110, 150, 300 and 450 °C), compaction pressure (250 and 320 MPa) and with two different substrate surface condition (smooth and roughened).

paction trials, the whole tooling was heated by a band heater (Watlow miniature band heater), and wrapped by insulation material to achieve and maintain the desired temperature levels while the temperature is continuously measured (K type thermocouples) and controlled by a temperature controller (Omega CN616, Fig. 4b). The insert (i.e., punch with the micro-channel features as seen in Fig. 4c) was fabricated using wire EDM process. As seen in Fig. 4c, the insert has a diameter of 10 mm with identical channel width of 435 μm and channel gap of 350 μm on the left side (i.e., aspect ratio is 0.8), and identical channel width of 400 μm and channel gap of 200 μm on the right side (aspect ratio is 0.5). Furthermore, there is a draft angle of around 14° on left side.

During the experiments, a thin copper substrate of Cu 110 alloy (100 μm thickness) was placed on the bottom die. Copper powders (Grade 185E, ACu Powder Co., water atomized) were poured on to it. Powders had irregular shapes and showed a large variation in their size (10% < 25 μm, 50% < 50 μm and 90% < 100 μm). The entire system was then heated to the required temperature level. Then, punch (insert) was pushed down by the MTS machine to the desired loading level. Depending on the type of experiments, the specimen was kept under certain pressure level for a while, which will be explained later. Then, the entire system was cooled down to room temperature to allow the formed specimen to be taken out of the die for further observations and measurements.

2.2. Experimental method

Table 1 summarizes the experimental conditions for Phases 1, 2 and 3 experiments. In the first set of experiments (Phase 1), we investigated the effect of temperature at high compaction pressure levels and for smooth and rough substrate surface conditions. As described above, at least three specimens were fabricated at 20, 110, 150, 300 and 450 °C under both 250 and 320 MPa levels. In the second set of experiments (Phase 2), we investigated the effect of compaction pressure and holding time at high temperature conditions. We performed at least three

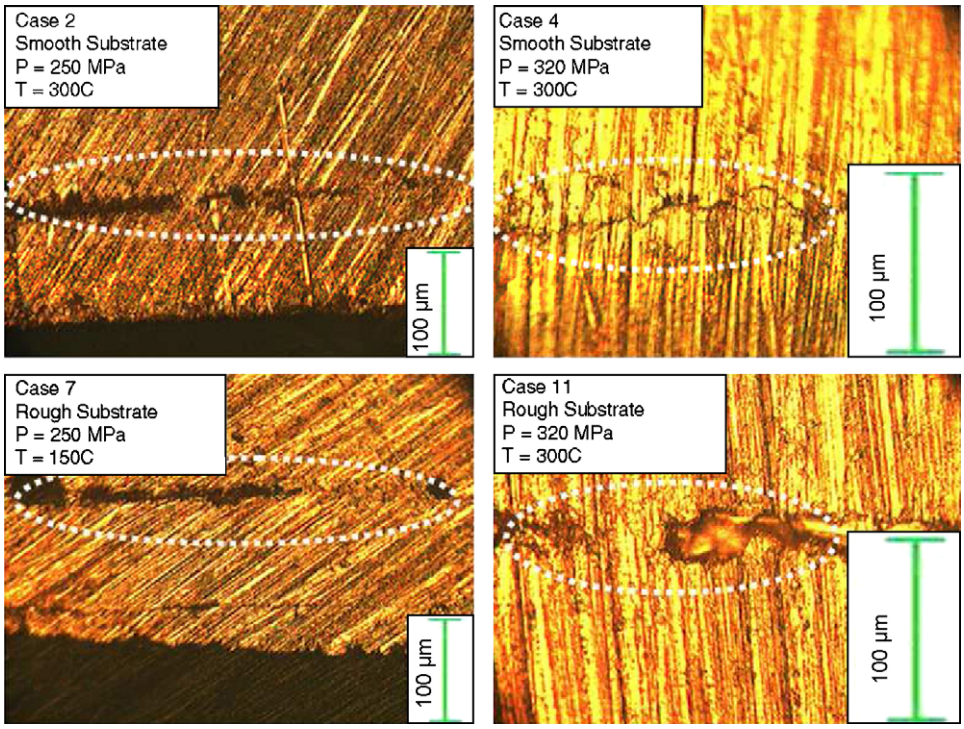

Fig. 9. Bonding with the thin substrate is one of the main requirements of such micro-scale porous surface structures. Only at high temperature levels of 300 and 450 °C, bonding was observed to take place.

compactions at 50, 70, 100, 150 and 200 MPa pressure levels under both 300 and 450 °C. We hold the compaction load at 30, 60 and 120 s to understand if it would make any difference in terms of the porosity and channel height. Finally, in the Phase 3-experiments, we only conducted hot compaction of more uniform powders (i.e., 90% was higher than 50 μm) at 450 °C and under 50 MPa to understand if powder size distribution would affect the porosity and cavity filling characteristics.

2.3. Measurements

In order to characterize the fabricated porous specimens, we performed two main measurements on every specimen: (1) channel height to understand the cavity/channel filling performance, (2) porosity to establish a relation between forming conditions (pressure, temperature, etc.) and porosity control. In this study, we did not perform any measurements to quan-

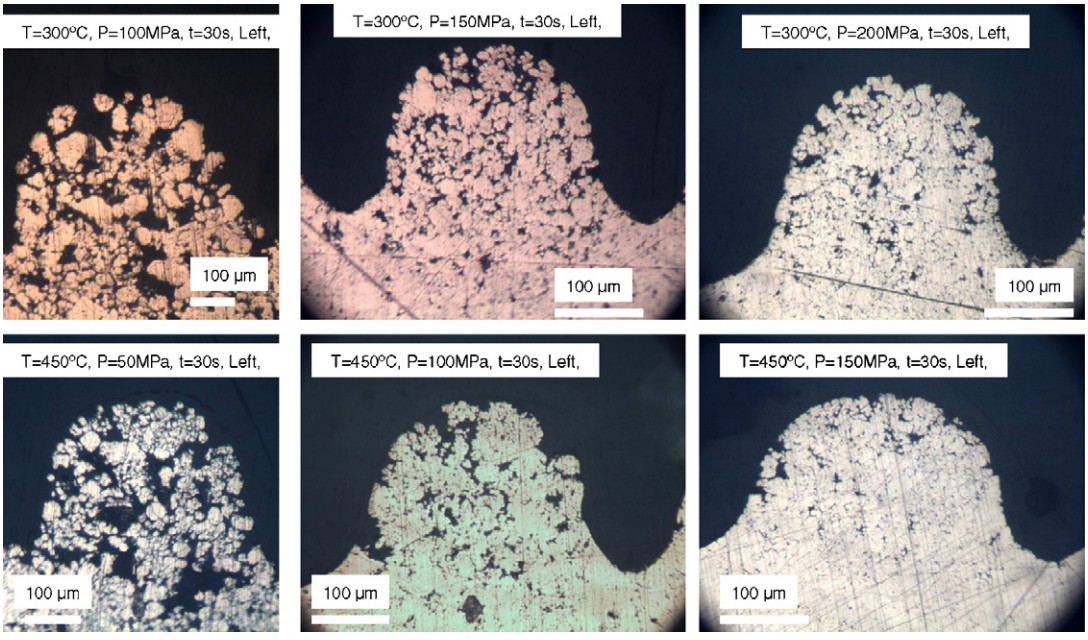

Fig. 10. Optical microscopy pictures of porous features at different temperature and pressure conditions.

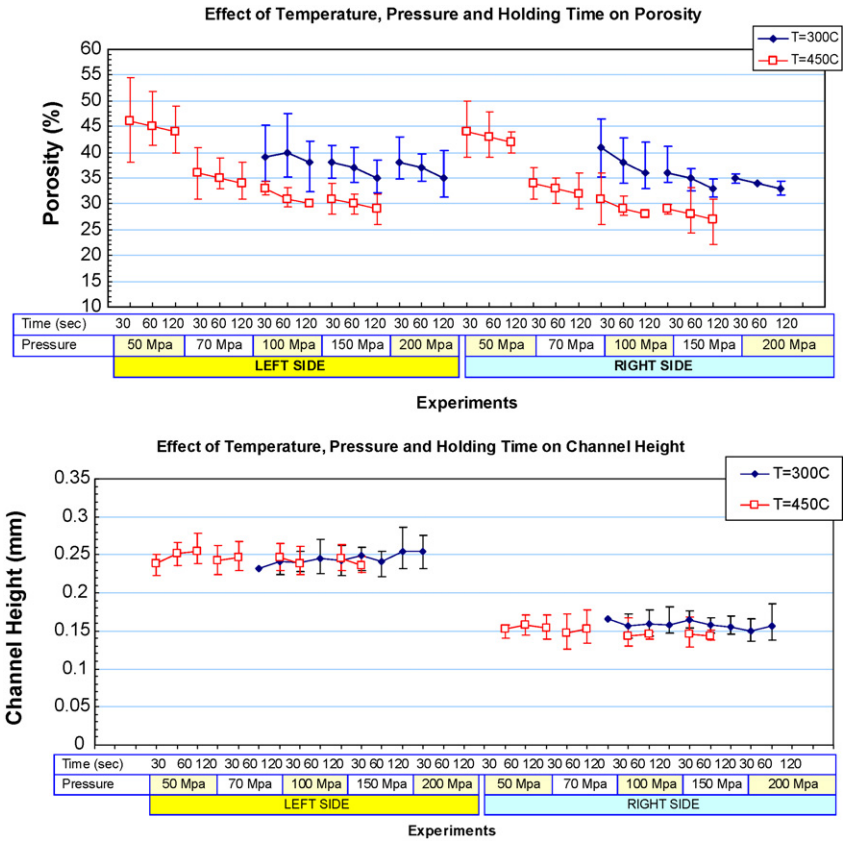

Fig. 11. Variation of porosity (a) and channel height (b) under different compaction conditions (temperature levels are 300 and 450 °C, pressure levels are 50, 70, 100, 150 and 200 MPa, holding times are 30, 60 and 120 s). Note that some of the cases were not performed.

tify the bond strength between substrate and porous layer. But, we examined it under microscope to understand its characteristics.

2.3.1. Channel height measurements

We used two different methods to measure the channel height on the fabricated specimens (Fig. 5). First, optical microscopy images were captured for the purpose of measuring porosity and specimen profile. We used Motic Image Processing Software to analyze the images. As a second method, we used a laser profiler (Keyence LK-G37, accuracy of 0.05 μm) which offers a faster measurement method. In order to ensure its accuracy and repeatability, we compared its results with optical microscopy images. As depicted in Fig. 6, laser profiling was found to give consistent measurements as good as optical microscopy imaging. For every fabricated specimen, we measured the channel height along two different lines as illustrated in Fig. 5. In the comparison charts, an average of these measurements was used.

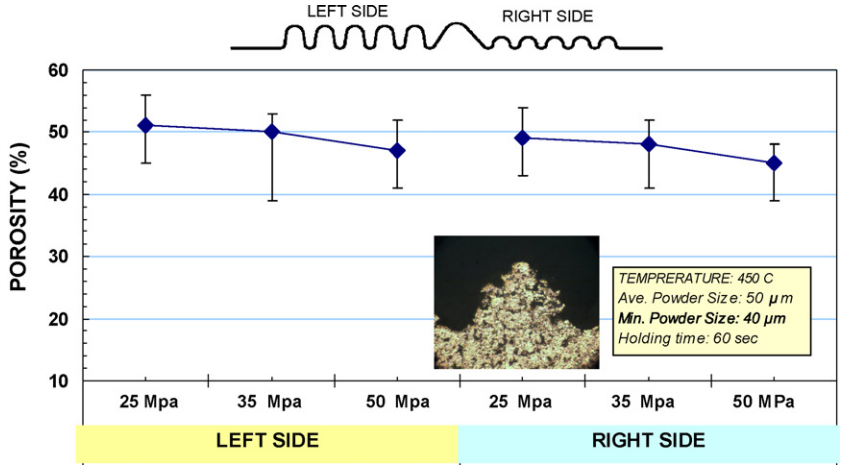

Fig. 12. Porosity levels at different pressure levels at a temperature of 450 °C using more uniform powders.

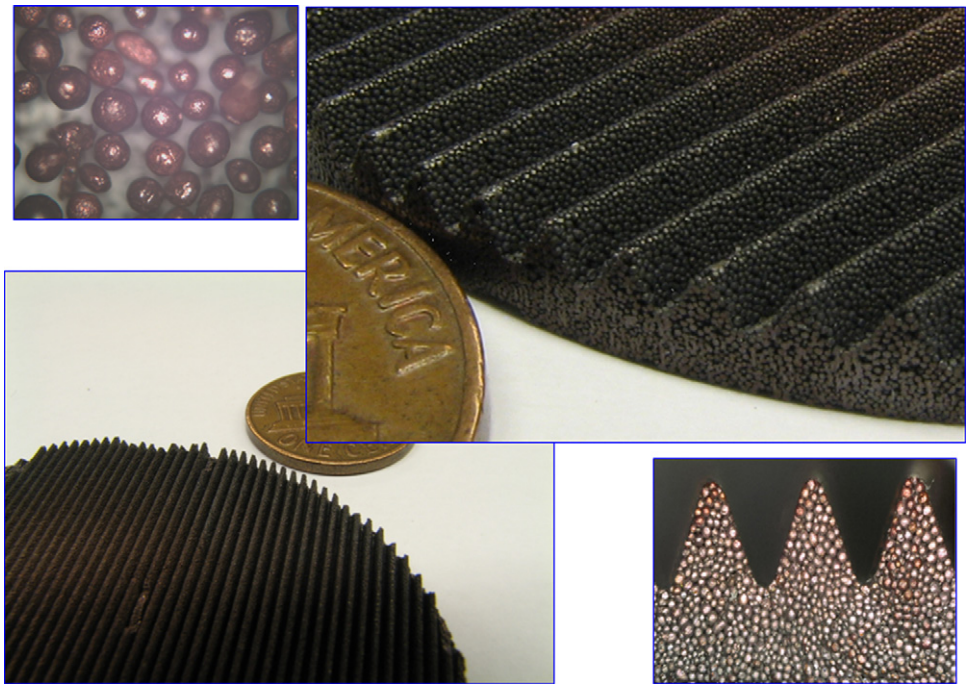

Fig. 13. Preliminary results of hot compaction with a new and large tooling.

2.3.2. *Porosity measurements*

In order to measure porosity level and distribution, we analyzed the optical microscopy images using image analyzing software, since it offered a rapid and accurate characterization of porosity and its distribution. In our characterization procedure, first the fabricated specimens were mounted to safeguard them from breaking or falling apart due to weaker bonding between powders. The mounted specimens were then cut into sections which then underwent grinding and polishing. Grinding was done using meshes of 240, 400, 800 and 1200 graded

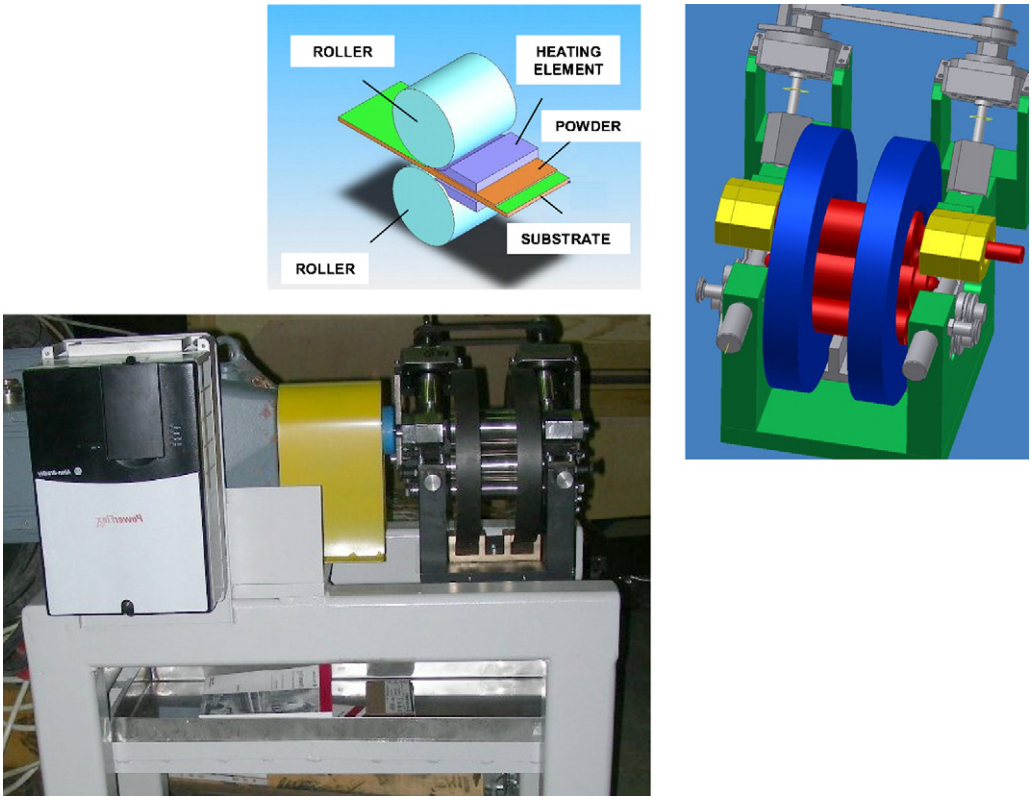

Fig. 14. Roll mill to perform continuous roll compaction of porous micro-feature surface structures.

sand paper consecutively and polishing was done using 6 and 1 μm grade diamond paste in order to obtain better quality surface images. Polished specimens were then examined under an optical microscope to capture multiple images in every section. These images were analyzed in both ImageJ and Motic Image Processing Software to quantify the porosity level and depict the porosity distribution. At least three distinct regions from each feature/channel on every section were used to obtain porosity measurement windows as illustrated in Fig. 7. An average of all these measurements was used in comparison and analyses.

3. Results, analysis and discussions

As explained before, complete characterization of porous surface structures requires comparison of (a) achievable channel/feature height/size, (b) attainable porosity (%), (c) strength (i.e., hardness) and (d) quality of bonding with the substrate. In this feasibility study, the focus of our investigations was on the first two attributes of the porous surfaces. Hence, in this section, we present and discuss the effects of pressure, temperature, substrate surface, feature size and powder size on the porosity (%) and feature height (h).

3.1. Results of Phase 1 experiments

In the Phase 1 experiments, we investigated the effect of temperature on the porosity and channel height and relatively high compaction pressure levels (250 and 320 MPa). Fig. 8 depicts the variation of porosity and channel height. It can be concluded that porosity decreases with increasing temperature from 35–40% levels down to 13–20% levels. It demonstrates about 2% increase in porosity when we go from 300 to 450 °C temperature, which could be neglected due to the large variation in measurements. Similarly, a decrease of porosity is observed with an increase in the pressure. However, at these two high-pressure levels of comparison, their effect on porosity is not very significant (i.e., 3–5%). Although insignificant, rough substrate causes a slight increase in porosity (i.e., in the range of 1–2%). Similar observations are made for both sides of the compaction specimen where aspect ratio is 0.8 and 0.5 on left and right sides, respectively. For the channel height comparisons, it is difficult to make general conclusions unlike the porosity. For both sides of the compacted specimens and for both pressure levels, the highest channel height is observed at a temperature of 110 and 450 °C, whereas the lowest height is obtained at 150 °C. Since, the compacted specimen is not strong enough at 20, 110 and 150 °C cases, they were susceptible for damage during ejection and handling. Bonding with substrate was not very strong, sometime not possible, at low temperature level as illustrated in Fig. 9. As summary, in order to obtain high porosity, high filling and strong compaction, we need to use a high temperature level. However, since it would be expensive, slow and difficult to conduct compaction at much high-temperatures, in the Phase 2 experiments, we investigated the effect of pressure at 300 and 450 °C temperature.

3.2. Results of Phase 2 experiments

In the second set of experiments, we focused on the effect of low-pressure levels and holding time on the porosity and height at high temperature conditions (i.e., 300 and 450 °C). We conducted compaction experiments at five different pressure levels (50, 70, 100, 150 and 200 MPa). We applied the final pressure level at different holding durations (30, 60 and 120 s). Fig. 10 illustrates the porosity and its distribution on several micro-features under different process conditions while Fig. 11 depicts the variation of average porosity and channel height. In general, the lower the temperature and pressure is, the higher the porosity.

Based on observations and depiction in Fig. 11, it can be concluded that pressure (between 50 and 200 MPa), temperature (300 and 450 °C) and holding time (30–120 s) have significant effect on the porosity but negligible impact on the channel height. Porosity decreases with increasing temperature to 450 °C from 300 °C. The rate of change is in the range of 7–10%. Increasing pressure also leads to a decrease in the porosity. Lower pressure (50 MPa) results in porosity around 40–45% while the higher pressure (200 MPa) leads to porosity about 32–35%. It should be noted that porosity decreases interruptedly between 50 and 70 MPa from 40–45% down to 30–35%. Holding time also affects the porosity by reducing it with longer holding durations, but its effect is not as pronounced as that of pressure and temperature. Finally, it can be deduced from these results that as the temperature and pressure increases, porosity variation on the same specimen decreases.

3.3. Results of Phase 3 experiments

In the Phase 3 experiments, the goal was to understand if the powder size uniformity had an effect on the attainable porosity. Hence, we screened the powder used in other phases to have a more uniform powder size distribution (i.e., as received powders had as distribution of 10% < 25 μm, 50% < 50 μm and 90% < 100 μm, whereas after screening we had powders of 45–53 μm, 270–320 mesh). We performed the Phase 3 tests under the following conditions: pressure: 25, 35 and 50 MPa, temperature: 450 °C, holding time: 60 s and using rough substrate. As it can be seen in Fig. 12, and after a comparison with Fig. 11a, it can be concluded that uniform powders lead to higher and more consistent porosity percentages (i.e., 45–50% at 50 MPa in Fig. 12 versus 40–45% in Fig. 11a at 50 MPa), as expected.

4. Conclusions and future work

The ultimate goal of this study was to verify the feasibility of fabricating porous micro-channels on large surfaces in a continuous manner. We hypothesized that micro-channels of around 200–400 μm height and width with porosity levels of 30–50% and with strong bonding to a thin substrate could be fabricated using hot powder compaction and/or hot roll powder compaction. Therefore, we investigated the effects of compaction pressure, temperature, holding time, powder size

and substrate conditions on the attainable porosity and channel size.

In summary, we conclude the followings:

(1) Porous micro-channels can be fabricated on large surfaces for fuel cell, fuel processor and other heat exchanger applications using copper, stainless steel and other metallic alloys.
(2) In order to ensure strong bonding among powders and between powders and substrate, temperature should be kept as high as possible (minimum of 450–500 °C for copper).
(3) Sintering would be necessary if temperature during compaction is not around 900–1000 °C.
(4) Both compaction and sintering should be performed under protected atmosphere to prevent oxidation.
(5) Pressure levels can be selected based on the achievable temperature levels. At high temperature levels such as above 450 °C, low-pressure values should be enough for compaction, but would require sintering process. Although high temperature and high pressure would assist in obtaining strong compactions, it would prevent reaching the necessary porosity levels.
(6) In order to ensure high and consistent levels of porosity, uniform powders should be used.
(7) Temperature gradient can be used to increase bond strength (i.e., high temperature at substrate and low temperature at channel side).

As future and recommended work, similar experiments need to be conducted for large scale and continuous compactions. We have already designed a new tooling to fabricate compactions of 55 mm in diameter and with larger aspect ratios (0.84 and 1.68) as presented in Fig. 13. In addition, design of experiment (DoE) techniques will be applied to obtain interacting effect of different parameters on the porosity. In order to understand the bond quality, shear and/or three-point tests are planned for quantitative characterization. We plan to transfer our findings from simple compaction case to roll compaction process. For this purpose, a specially designed roll mill is acquired as shown in Fig. 14. As for the second phase of this study, we plan to use stainless steel powders to make interconnect/bipolar plate samples for fuel cell applications. It is obvious that for stainless steel powders, we would need to conduct our compaction experiments under higher temperature (600–800 °C) and pressure (∼100 MPa) levels in order to obtain sound bonding among powders and between powders and substrate.

Acknowledgements

Authors are thankful to National Science Foundation (NSF) for the partial support on this project through NSF ENG/CMMI Grant 0638522. We also acknowledge technical and financial support of Luvata Co. for providing the specially designed roll mill for our future studies, and sharing their existing heat exchanger fabrication information. We are thankful to Dr. Steve Wayne, former CEO of Advanced Heat Transfer, LLC; and Prof. Masoud Kaviany of University. of Michigan for supporting us with their invaluable and in-depth knowledge on heat/mass transfer in porous media.

References

[1] M. Abdelhamid, Y. Mikhail, Stainless steel as a bipolar plate material in PEM fuel cell environments: stability issues, in: Proceedings of Annual Conference of American Institute of Chemical Engineering, New Orleans, LA, March 13, 2002.
[2] R. Bar-On, R. Kirchain, R. Roth, J. Power Sources 109 (1) (2002) 71–75.
[3] A. Heinzel, F. Mahlendorf, O. Niemzig, C. Kreuz, J. Power Sources 131 (2004) 35–40.
[4] N.P. Brandon, D. Corcoran, D. Cummins, A. Duckett, K. El-Khoury, D. Haigh, R. Leah, G. Lewis, N. Maynard, T. McColm, R. Trezona, A. Selcuk, M. Schmidt, J. Mater. Eng. Perform. 13 (3) (2004)253.
[5] M. Tucker, G. Lau, C. Jaconson, L. Delonghe, S. Visco, Stability of metal-supported SOFCs, in: Fuel Cell Seminar Abstracts, San Antonio, TX, USA, October 15–19, 2007, 215 pp.
[6] J. Scherer, R. Stroebel, B. Gaugler, C. Schleier, R. Glueck, W. Berroth, Mass manufacturing of metallic bipolar plates for PEFC – on the way to high quality low cost products, in: Proceedings of the 2007 Fuel Cell Seminar, San Antonio, TX, USA, October 16–19, 2007, pp. 166–169.
[7] R.H. Blunk, D.J. Lisi, Y.E. Yoo, C.L. Tucker, AIChE J. 49 (2003) 18–29.
[8] K. Butcher, et al., Scale-up of carbon/carbon composite bipolar plates, in: Proceedings of Annual Conference of American Institute of Chemical Engineering, New Orleans, LA, March 13, 2002.
[9] E.A. Cho, U.-S. Jeon, H.Y. Ha, S.-A. Hong, I.-H. Oh, J. Power Sources 125 (2004) 178–182.
[10] B. Cunningham, D.G. Baird, J. Mater. Chem. 16 (2006) 4385–4388.
[11] J. Banhart, JOM 52 (12) (2000) 22–27.
[12] J. Banhart, Prog. Mater. Sci. 46 (2001) 559–632.
[13] G.J. Davies, S. Zhen, J. Mater. Sci. 18 (1983) 1899–1911.
[14] S.G. Liter, M. Kaviany, Int. J. Heat Mass Transfer 44 (22) (2001) 4287–4311.
[15] J. Larminie, A. Dicks, Fuel Cell Systems Explained, second ed., John Wiley and Sons Ltd., England, 2003.
[16] A. Bose, Adv. Powder Metall. Particulate Mater. 2 (1996) 5259–5273.
[17] P.S. Liu, K.M. Liang, J. Mater. Sci. 36 (21) (2001) 5059–5072.
[18] M. Fuji, E. Nishiyama, G. Yamanaka, Advances in Enhanced Heat Transfer, vol. 18, ASME, New York, 1979, pp. 45–51.
[19] S.P. Malyshenko, Therm. Eng. 38 (2) (1991) 81–88 (English translation of Teploenergetika).
[20] R.M. Milton, Heat exchange system, U.S. patent 3,384,154 (1968).
[21] G.T. Kartsounes, ASHRAE Trans. 81 (1) (1975) 320–326.
[22] M.M. Dahl, L.D. Erb, Liquid heat exchanger interface and method, U.S. patent 3,990,862 (1976).
[23] K.R. Janowski, M.S. Shum, S.A. Bradley, Heat transfer surface, U.S. patent 4,129,181 (1978).
[24] T. Kunugi, K. Muko, M. Shibahara, Superlattices Microstruct. 35 (3–6) (2004) 531–542.
[25] H.I. Bakan, Scripta Mater. 55 (2006) 203–206.
[26] N. Cunningham, et al., J. Electrochem. Soc. 149 (7) (2002) A905–A911.
[27] B. Matijasevic, J. Banhart, Scripta Mater. 54 (4) (2006)503–508.